α₁-Adrenergic receptors prevent a maladaptive cardiac response to pressure overload

Timothy D. O'Connell,[1,2] Philip M. Swigart,[1] M.C. Rodrigo,[1,2] Shinji Ishizaka,[3]
Shuji Joho,[3] Lynne Turnbull,[1,4] Laurence H. Tecott,[5] Anthony J. Baker,[1,4]
Elyse Foster,[3] William Grossman,[3] and Paul C. Simpson[1,2]

[1]Cardiology Division, San Francisco Veterans Affairs Medical Center, San Francisco, California, USA. [2]Cardiovascular Research Institute and
Department of Medicine, UCSF, San Francisco, California, USA. [3]Cardiology Division, Department of Medicine, UCSF, San Francisco, California, USA.
[4]Department of Radiology, UCSF, San Francisco, California, USA. [5]Department of Psychiatry, UCSF, San Francisco, California, USA.

An α₁-adrenergic receptor (α₁-AR) antagonist increased heart failure in the Antihypertensive and Lipid-Lowering Treatment to Prevent Heart Attack Trial (ALLHAT), but it is unknown whether this adverse result was due to α₁-AR inhibition or a nonspecific drug effect. We studied cardiac pressure overload in mice with double KO of the 2 main α₁-AR subtypes in the heart, α₁A (*Adra1a*) and α₁B (*Adra1b*). At 2 weeks after transverse aortic constriction (TAC), KO mouse survival was only 60% of WT, and surviving KO mice had lower ejection fractions and larger end-diastolic volumes than WT mice. Mechanistically, final heart weight and myocyte cross-sectional area were the same after TAC in KO and WT mice. However, KO hearts after TAC had increased interstitial fibrosis, increased apoptosis, and failed induction of the fetal hypertrophic genes. Before TAC, isolated KO myocytes were more susceptible to apoptosis after oxidative and β-AR stimulation, and β-ARs were desensitized. Thus, α₁-AR deletion worsens dilated cardiomyopathy after pressure overload, by multiple mechanisms, indicating that α₁-signaling is required for cardiac adaptation. These results suggest that the adverse cardiac effects of α₁-antagonists in clinical trials are due to loss of α₁-signaling in myocytes, emphasizing concern about clinical use of α₁-antagonists, and point to a revised perspective on sympathetic activation in heart failure.

Introduction

α₁-Adrenergic receptors (α₁-ARs) are G protein–coupled receptors activated by the endogenous catecholamines norepinephrine and epinephrine. α₁-ARs were discovered through their physiological effect to increase smooth muscle contraction, and α₁-AR antagonist drugs are used commonly to treat disorders with increased smooth muscle contraction, such as hypertension and prostate enlargement with urinary symptoms. However, more recent studies find α₁-ARs in the heart and document a variety of beneficial cardiac effects of myocyte α₁-AR stimulation, including physiological hypertrophy, preconditioning, protection from apoptosis, and increased contractility (1–4). If α₁-signaling has an adaptive role in cardiac myocytes, then α₁-antagonist drugs might have negative side effects on the heart.

One arm of the Antihypertensive and Lipid-Lowering Treatment to Prevent Heart Attack Trial (ALLHAT) in hypertension tested the α₁-antagonist doxazosin versus the diuretic chlorthalidone in 24,335 men and women with cardiac risk factors (5). This arm of the trial was stopped prematurely, because doxazo-

sin doubled the incidence of heart failure, and further detailed analyses indicated a doxazosin effect to increase heart failure that was not seen with other antihypertensive medications (5–8). Similarly, in the Vasodilator–Heart Failure Trials (V-HeFT), the α₁-antagonist prazosin did not improve survival as did other vasodilators and even tended to increase mortality (9). Doxazosin and prazosin are piperazinyl quinazolines, which at high doses can cause apoptosis in heart and other tissues independent of α₁-ARs (10, 11), and also have relatively high affinity for α₂-AR subtypes B and C (12, 13). Thus, it remains controversial whether the adverse results in the ALLHAT and V-HeFT trials were due to α₁-AR inhibition itself, or a nonspecific drug effect. This question has important therapeutic implications, given the large number of patients treated with α₁-antagonists for hypertension or prostate disease. Indeed, a recent editorial suggested that over 7 million American men aged 65 and over with prostate enlargement would benefit from this type of drug (14).

Recently, we characterized a mouse with double KO of the 2 main α₁-AR subtypes, α₁A and α₁B (*Adra1a* and *Adra1b*), named the ABKO mouse (1). The ABKO eliminated heart α₁-AR binding, decreased myocardial and myocyte Erk activity, and markedly reduced physiological heart and myocyte hypertrophy during postnatal development. In addition, the ABKO mouse had reduced survival after pressure overload by transverse aortic constriction (TAC) (1).

In the current study, we examined the response to pressure overload in ABKO mice. The TAC model of pressure overload magnifies a pathological stimulus that simulates hypertension in patients, and compresses the stimulus into a short time. We
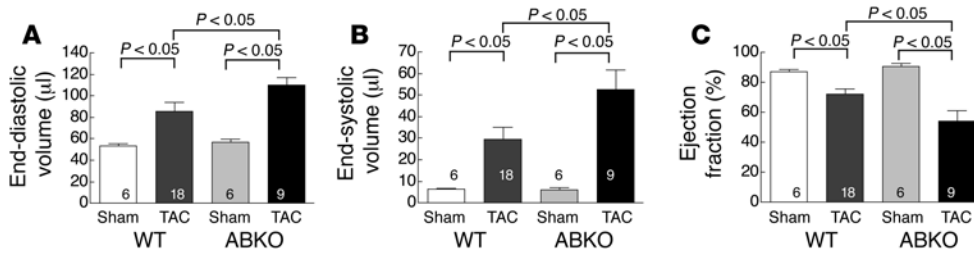
Figure 1
Dilated cardiomyopathy after TAC by echocardiography. Conscious mice were studied 2 weeks after TAC or sham operation. Ventricular volumes (**A** and **B**) were calculated by the cubed method (volume = 1.047 × LV internal dimension^3), where LV internal dimension is defined as the distance between the LVFW and the IVS on a 2-dimensionally guided M-mode echocardiogram, and ejection fraction (**C**) was determined by the formula (end-diastolic volume – end-systolic volume)/end-diastolic volume × 100 (85, 86). Numbers of mice are indicated.

find that double KO of the α_{1A}- and α_{1B}-ARs worsens dilated cardiomyopathy after pressure overload, and we identify several potential cellular mechanisms of maladaptation, all of which can be related to the loss of α_1-ARs in cardiac myocytes. These results show that α_1-signaling is required for cardiac adaptation and caution against the use of α_1-antagonist drugs. The results also provide a potential explanation for the recent surprising adverse effects of sympathetic blockade in heart failure (15–18) and thus suggest that the current neurohormonal paradigm in heart failure, that all sympathetic activation is harmful and should be blocked, might not be correct.

Results

Worse dilated cardiomyopathy after TAC in the ABKO. To test whether α_1-ARs were required for an adaptive response to pathological pressure overload, we performed TAC on adult male, congenic, WT and ABKO mice, which have no detectable α_1-AR binding in the heart (1). As reported previously in a somewhat smaller cohort (1), survival to 2 weeks after TAC was markedly reduced in the ABKO (61%, 11 of 18, $P < 0.05$) versus WT (100%, 18 of 18), or versus sham-operated mice of either genotype (100%, 6 of 6). ABKO mice died at 5–8 days after TAC, with signs of heart failure at autopsy (1). Pressure gradients at 2 weeks after TAC were not significantly different (WT, 98 ± 5, $n = 18$; ABKO, 108 ± 8, $n = 11$, $P = $ NS), indicating that imposed loads were similar. Thus, deletion of α_1-ARs caused a highly maladaptive response to pressure overload.

To test for maladaptive remodeling in the ABKO after TAC, we studied mice that survived at least 2 weeks, using echocardiography in conscious mice. In WT mice, TAC caused decreased ejection fraction ($P < 0.05$ versus WT sham-operated mice) and increased end-diastolic and end-systolic volumes ($P < 0.05$), demonstrating pathological ventricular remodeling (Figure 1, A–C, and Table 1). In surviving ABKO mice after TAC, ejection fraction was decreased even further (77% of WT TAC ejection fraction, $P < 0.05$), and end-diastolic and end-systolic volumes were even larger (128% and 183% of WT TAC volumes, $P < 0.05$). In addition, lung weight/body weight ratio, an index of heart failure, tended to increase in surviving ABKO mice after TAC (193% versus sham, 143% versus WT TAC, both $P = 0.1$). In summary, the ABKO mice that survived 2 weeks had a worse dilated cardiomyopathy after TAC.

Remodeling after TAC in ABKO mice that survived or died. To test whether the ABKO mice that died after TAC had a phenotype different from that of the ABKO mice that survived, we did seri-

al echocardiography in conscious mice. Echocardiograms were obtained before TAC and at days 3 and 7 after TAC in a cohort of 8 male ABKO mice. Four of these ABKO mice died between 1 and 3 weeks after TAC (50% mortality). As shown in Figure 2, development of dilated cardiomyopathy during the first week after TAC was the same in the 4 ABKO mice that ultimately died, as compared with the 4 ABKO mice that survived, with a significant decrease over time in ejection fraction, and significant increases in LV volumes (Figure 2, A–C). Extension of the curves for an additional week would produce values very similar to those of the ABKO survivors at 2 weeks, shown in Table 1. Heart rate and cardiac output tended to be lower in ABKO mice that later died ($P = $ NS; Figure 2, D–F). The pressure gradient was identical in the dying and surviving groups (Figure 2G) and increased with time after TAC, as reported previously (19). Because ABKO mice typically died at night, we could not determine whether death was due to progressive heart failure or arrhythmia, but some mice had fluid in the body cavities at autopsy, indicating heart failure. In patients with heart failure in clinical trials, similar to the ABKO mice, some survive and some do not, despite equally low ejection fractions and enlarged LV volumes (20–22). In summary, these data suggested that both dead and surviving ABKO mice had a similar phenotype. Therefore, we considered worse dilated cardiomyopathy to be the major abnormality in the ABKO after pressure overload, and we studied the cellular mechanisms of cardiomyopathy in ABKO mice that survived 2 weeks.

Heart and myocyte size after TAC. One potential mechanism for worse dilated cardiomyopathy in the ABKO after TAC was "inadequate hypertrophy," or failure of heart and myocyte size to increase sufficiently. Increased size is thought to be an adaptive response to increased afterload, and inadequate hypertrophy causing heart failure is observed in some animal models and in humans (23–25). However, as shown in Figure 3A and Table 1, both the ABKO and the WT mice had significant hypertrophy after TAC, and final heart weight/body weight ratio (HW/BW) was the same in the 2 genotypes. In fact, because baseline HW/BW was smaller in the ABKO mouse than in the WT ($P < 0.05$; see sham in Figure 3A and Table 1), confirming our previous report (1), the percentage increase in HW/BW was even greater in the ABKO (179% in ABKO versus 152% in WT). Myocyte cross-sectional area, an index of myocyte size, mirrored the changes in HW/BW (Figure 3B and Table 1). In summary, the worse dilated cardiomyopathy in the ABKO was not due to an inadequate increase in heart or myocyte size per se.

Fibrosis after TAC. The hypertrophic response to a pathological stimulus often includes increased fibrosis (26). Fibrosis detected by Sirius red staining for collagen was negligible in hearts from sham-operated ABKO and WT mice (Table 1). In TAC hearts, interstitial fibrosis and perivascular fibrosis were prominent. Interstitial fibrosis in WT hearts after TAC was 7–10% of the

Table 1
Echocardiography and pathology after TAC

	WT			ABKO			KO/WT (%)	
	Sham	TAC	TAC/Sham (%)	Sham	TAC	TAC/Sham (%)	Sham	TAC
Echocardiography								
n	6	18		6	9			
EDV (µl)	53 ± 2	86 ± 8	162[A]	57 ± 3	110 ± 7	193[B]	107	128[C]
ESV (µl)	6 ± 0	29 ± 6	483[A]	6 ± 1	53 ± 9	883[B]	100	183[C]
SV (µl)	47 ± 2	56 ± 2	119	51 ± 2	58 ± 5	114	108	104
HR (bpm)	716 ± 6	664 ± 15	93	694 ± 7	600 ± 20	86[B]	97	90[C]
CO (ml/min)	34 ± 2	37 ± 1	109	35 ± 2	35 ± 3	100	103	95
EF (%)	88 ± 1	70 ± 3	79[A]	90 ± 1	54 ± 6	60[B]	102	77[C]
PG (mmHg)		98 ± 5			108 ± 8			110
Pathology								
BW	25 ± 1 (5)	29 ± 1 (10)	116	24 ± 1 (4)	28 ± 2 (11)	117	96	97
HW/BW	5.0 ± 0.1 (5)	7.6 ± 0.7 (10)	152[A]	4.6 ± 0.2 (4)	8.2 ± 1.0 (11)	178[B]	92[D]	108
MC CSA (µm²)	162 ± 30 (3)	345 ± 54 (6)	213[A]	105 ± 5 (3)	297 ± 75 (4)	283[B]	65[D]	86
Lung wt/BW	6.6 ± 0.2 (5)	8.4 ± 1.3 (10)	127	6.2 ± 1.0 (4)	12.0 ± 2.3 (8)	193	94	143
Fibrosis (% area)								
LVFW	0	10 ± 2 (8)		0	26 ± 3 (4)			260[C]
IVS	0	7 ± 2 (8)		0	26 ± 9 (4)			371[C]
RV	0	2 ± 2 (8)		0	1 ± 1 (4)			50
mRNAs ($n = 3$)								
ANF	0.79 ± 0.1	5.70 ± 2.3	721	0.81 ± 0.2	1.86 ± 0.1	230	102	33
αMyHC	1.45 ± 0.1	1.28 ± 0.1	88	1.22 ± 0.0	0.91 ± 0.2	75	84	71
βMyHC	1.41 ± 0.2	6.60 ± 0.7	468[A]	1.19 ± 0.3	1.42 ± 0.2	119	84	22[C]
SERCA	1.58 ± 0.1	0.96 ± 0.2	61	0.99 ± 0.1	0.63 ± 0.2	64	63	66
SkAct	0.50 ± 0.1	3.25 ± 0.4	650[A]	0.34 ± 0.1	0.74 ± 0.2	218	68	23[C]
TUNEL (% cells)	0.06 ± 0.01 (3)	0.35 ± 0.03 (5)	583[A]	0.08 ± 0.04 (3)	1.31 ± 0.34 (4)	1638[B]	133	374[C]
PKCδ ($n = 3$)								
Full-length	107 ± 12	276 ± 25	257[A]	150 ± 11	359 ± 34	240[B]	140	130
Cleaved	75 ± 17	217 ± 21	290[A]	132 ± 4	312 ± 8	236[B]	176[D]	144[C]

Two-dimensionally guided M-mode echocardiography and pathology were done 2–4 weeks after TAC or sham surgery in ABKO and WT mice. The methods were as in the legends to Figures 1–5. EDV, end-diastolic volume; ESV, end-systolic volume; cardiac output (CO) = heart rate (HR) × stroke volume (SV); EF, ejection fraction; PG, pressure gradient across the TAC; MC CSA, myocyte cross-sectional area. Ventricle mRNA levels are density units normalized to 18S. Ventricle phospho-PKCδ levels are density units (× 10^{-3}) normalized to total protein. Values are mean ± SEM. The number of mice or hearts is given or in parentheses. $P < 0.05$ for [A]WT TAC versus sham, [B]ABKO TAC versus sham, [C]ABKO TAC versus WT TAC, and [D]ABKO sham versus WT sham.

area of the LV free wall (LVFW) endocardium and papillary muscle and the interventricular septum (IVS) base and midportion (Figure 3C and Table 1), similar to the findings of others in this model (27). In the ABKO TAC heart, interstitial fibrosis was increased to 26% of the LVFW and IVS, or 260% to 371% greater than in the WT TAC heart ($P < 0.05$). ABKO hearts also had a notable increase in interstitial fibroblasts in H&E-stained LV sections, but few inflammatory cells (white blood cells; data not shown). In contrast, perivascular fibrosis in ABKO and WT hearts was the same, averaging 25% of the area of microscopic fields containing intramural arteries with approximately 20 µm lumen diameter. In the nonloaded RV, fibrosis after TAC was low and was the same in both genotypes (Table 1). In summary, the ABKO heart after TAC had significantly greater LVFW and IVS interstitial fibrosis than the WT heart, but LV perivascular fibrosis and RV interstitial fibrosis were the same as in the WT.

Fetal gene induction after TAC. Pressure overload and other pathological stresses typically cause induction of the fetal hypertrophic gene program, which is correlated with pathological ventricular remodeling (28). In WT hearts, as expected, TAC robustly increased the mRNA levels of the fetal genes *atrial natriuretic factor* (*ANF*), β-*myosin heavy chain* (β*MyHC*), and α-*skeletal actin* (*SkAct*; Figure 4

and Table 1). In ABKO mice, in marked contrast, TAC did not induce β*MyHC* or *SkAct* (*P* = NS versus sham, *P* < 0.05 versus WT TAC) and increased *ANF* much less than in WT (Figure 4 and Table 1). Also, in the ABKO, TAC tended to decrease further the mRNAs for α*MyHC* and *sarcoplasmic reticulum calcium ATPase 2a* (*SERCA*; Figure 4 and Table 1). In summary, the ABKO impaired the transcriptional response to pressure overload.

Apoptosis in heart after TAC. We tested for apoptosis after TAC, since cell death by apoptosis has emerged as a causative factor in cardiomyopathy (29, 30). First, we used a TUNEL assay that gives approximately 100% nuclear labeling in positive controls treated with DNase (31). In WT hearts 2 weeks after TAC, apoptotic cells identified by TUNEL were increased by 583% versus hearts from sham-operated mice (*P* < 0.05; Figure 5, A and B, and Table 1). In ABKO hearts after TAC, apoptotic cells were further increased by 1,638% versus hearts from sham-operated mice (*P* < 0.05) and 374% versus hearts from WT TAC mice (*P* < 0.05). Hearts from sham-operated mice of both genotypes had the same numbers of apoptotic cells (Figure 5B).

Second, we tested for cleavage of PKCδ, a target for activated caspases in apoptosis. TAC for 1 week increased the protein levels of full-length phospho-PKCδ in ABKO and WT myocardium by
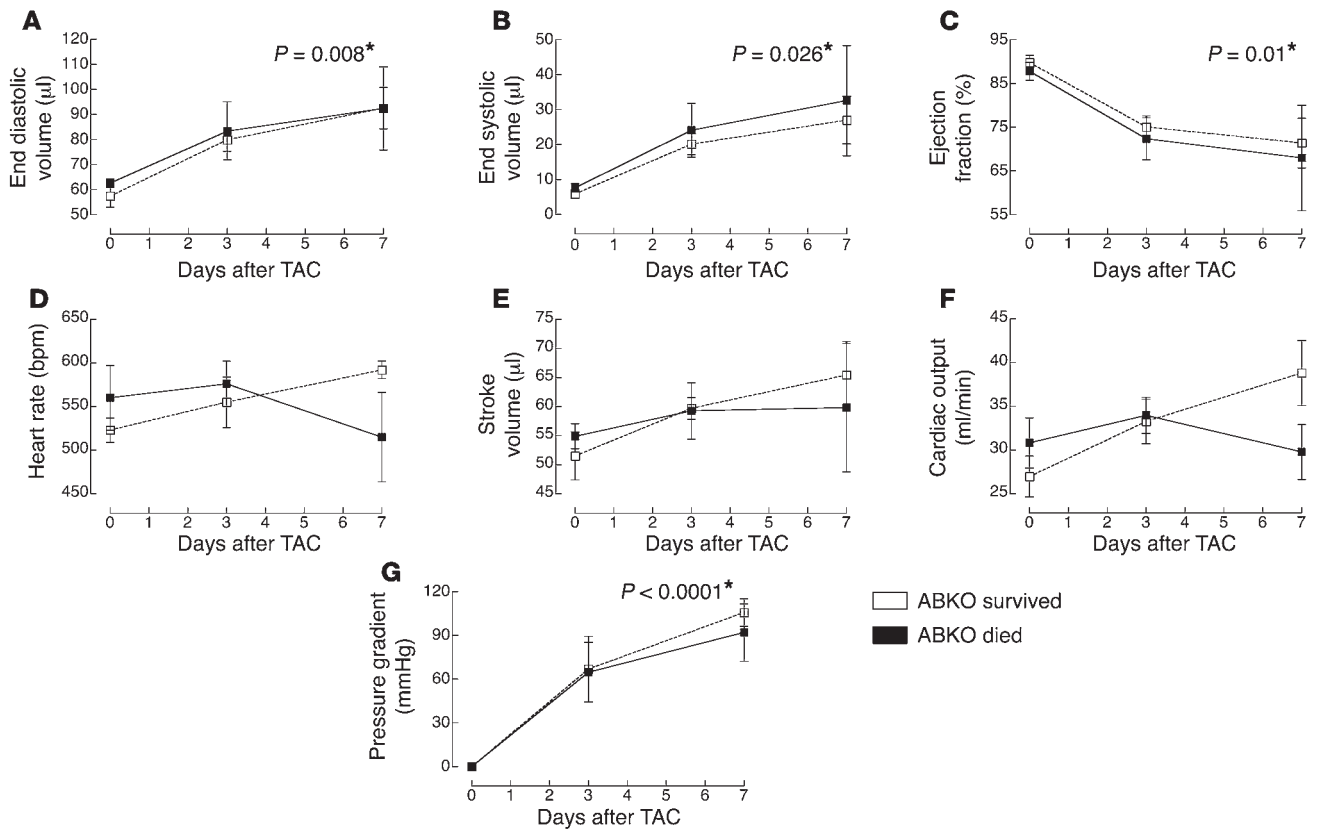
Figure 2
Remodeling in ABKO mice that survived and that died after TAC. Echocardiography was done on 8 conscious ABKO mice before TAC (day 0) and on days 3 and 7 after TAC. Of the 8 ABKO mice, 4 survived at least 3 weeks, and 4 died between 1 and 3 weeks. Echocardiography results from surviving and dying mice over the first week are shown and were compared by 2-way ANOVA. End-diastolic volume (**A**), end-systolic volume (**B**), ejection fraction (**C**), and pressure gradient (**G**) changed significantly over time in both groups (*P value given), but heart rate (**D**), stroke volume (**E**), and cardiac output (**F**) did not change. There were no significant differences between the 2 groups on any day.

257% and 240% versus the respective shams ($P < 0.05$; Figure 5C and Table 1). Others also see an increase in phospho-PKCδ levels after pressure overload (32). Cleaved phospho-PKCδ, presumed to reflect caspase activation, was somewhat higher in hearts from sham-operated ABKO mice (176% versus WT, $P < 0.05$). After TAC, cleaved PKCδ increased in both WT and ABKO hearts (290% and 236% versus their shams, $P < 0.05$), and the level of cleaved PKCδ was higher in the ABKO (144% versus WT TAC, $P < 0.05$; Figure 5C and Table 1). As observed by others (33), we saw cleavage of PKCδ in the ABKO cardiomyopathy (Figure 5C), but not cleavage of PARP (not shown). In summary, the ABKO heart had increased apoptosis after TAC by histological and biochemical criteria.

Apoptosis in cultured myocytes. To test whether ABKO myocytes were more susceptible to apoptotic stimuli that typically increase with pressure overload, which might explain increased apoptosis in ABKO hearts after TAC, and to be certain that apoptosis involved myocytes (Figure 5), we measured apoptosis in cardiac myocytes isolated from hearts not subjected to TAC. We treated cultured myocytes for 2 hours with reactive oxygen species (H_2O_2) and β-adrenergic catecholamines, both of which are increased in hypertrophy and heart failure (34–37), and assayed annexin V staining as an early marker for apoptosis. In WT cultures, annexin V–positive myocytes tended to increase with H_2O_2, norepinephrine (NE), and isoproterenol (ISO; 114%

to 145% versus vehicle, P = NS; Figure 6, A and B). In ABKO myocytes, apoptosis was the same as in WT with vehicle but increased much more than in WT with all apoptotic stimuli (207% to 249% versus vehicle, $P < 0.05$; 157% to 197% versus WT with the same stimulus, $P < 0.05$; Figure 6). In summary, ABKO myocytes were more susceptible than WT myocytes to apoptotic stimuli that are increased after pressure overload.

β-ARs in heart and myocytes. Increased apoptosis of ABKO myocytes with β-adrenergic catecholamines (Figure 6) raised the possibility of β-AR upregulation in ABKO myocytes. To test this, we measured β-AR levels and signaling in hearts and myocytes not subjected to TAC (Figure 7). ABKO hearts had no changes in β-AR binding normalized per mg protein, in the fraction of β2-ARs by competitive binding, or in β1 and β2 mRNAs by RNase protection (Figure 7A). The absolute values for β-AR binding in heart were 41 ± 3 fmol/mg protein for ABKO and 36 ± 2 for WT (n = 3; P = NS). The percentage β2 binding was 25% ± 4% for ABKO (n = 6) and 23% ± 6% for WT (n = 5, P = NS). The [125I]-cyanopindolol Kd was the same in ABKO (72 ± 18 pM) and WT (108 ± 22 pm; P = NS).

However, the isolated, perfused ABKO heart had marked desensitization (increase in EC50) of the ISO-stimulated increase in LV systolic pressure (LVSP) and decrease in LV end-diastolic pressure (LVEDP) (Figure 7, A, C, and D). In the isolated, perfused
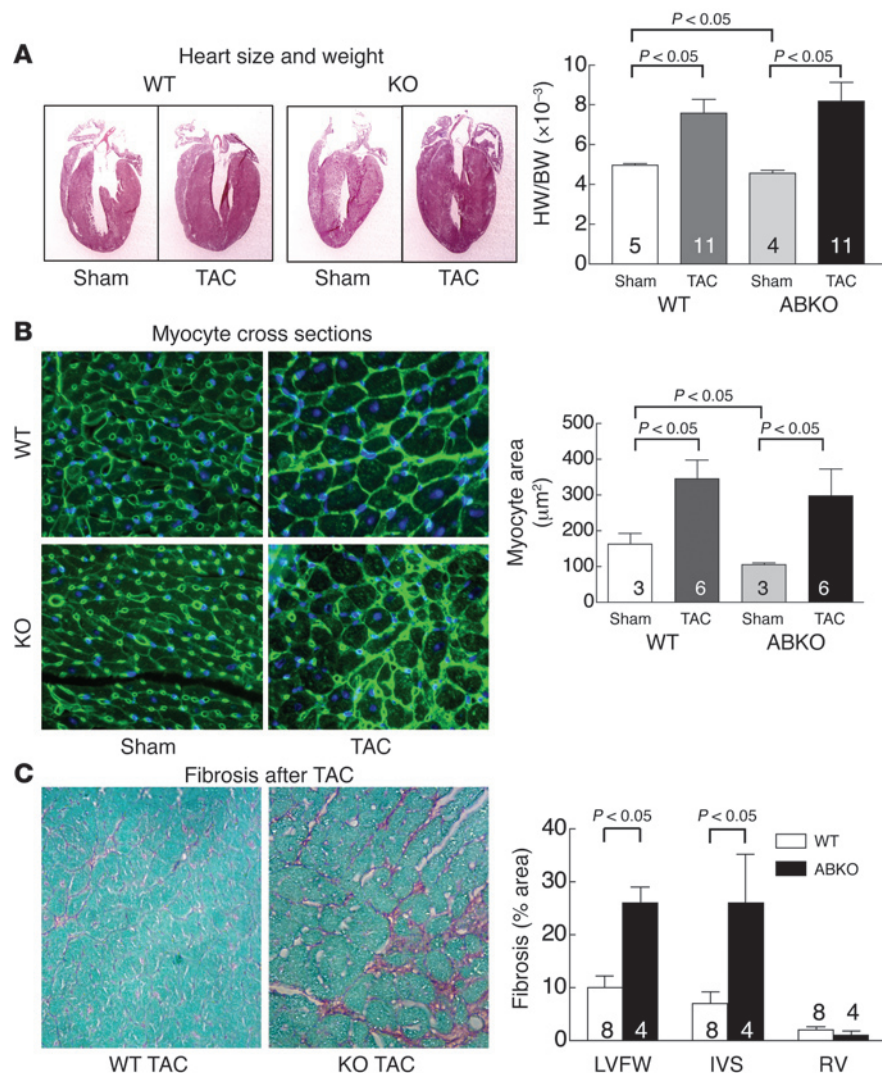
A

Heart size and weight

B

Myocyte cross sections

C

Fibrosis after TAC

Figure 3

Heart and myocyte size and fibrosis. Measurements were made 2 weeks after TAC or sham surgery. (**A**) Left: Heart coronal sections stained with H&E. Magnification, ×25. Right: Heart wet weight/body weight ratio (HW/BW). (**B**) Left: Ventricular sections stained with FITC-conjugated wheat germ agglutinin and Hoechst 33342. Magnification, ×400. Right: Myocyte cross-sectional area from at least 200 myocytes per heart in randomly selected fields. (**C**) Left: Ventricular sections stained with fast green and Sirius red for collagen. Magnification, ×400. Right: Interstitial fibrosis as a percentage of total microscopic area from at least 12–14 fields per heart. Numbers of hearts are indicated on the bars.

major protein kinase A site (38) (Figure 7B and data not shown). On the other hand, ABKO myocytes had no changes in β-AR binding per unit protein or in β-subtype mRNA levels per unit RNA (Figure 7B). The absolute values for β-AR binding in isolated myocytes as fmol per 6,000 cells were 10 ± 0.3 for ABKO and 19 ± 4 for WT ($n = 3$; $P < 0.05$), whereas the absolute values as fmol/mg protein were 18 ± 4 for ABKO and 19 ± 3 for WT ($n = 3$; $P = $ NS). The β_1- and β_2-AR proteins per mg of total myocyte protein were also unchanged by Western blot, although the protein bands were not consistently absent in the β-AR KO heart controls (data not shown). For β-AR mRNAs by quantitative RT-PCR, the mRNA molecules ($\times 10^{-9}$/50 ng RNA) were 14 ± 5 for β_1 ABKO and 12 ± 2 for β_1 WT; 14 ± 2 for β_2 ABKO and 10 ± 2 for β_2 WT; and 0.007 ± 0.001 for β_3 ABKO and 0.005 ± 0.002 for β_3 WT ($n = 3$; $P = $ NS). The percentages of each subtype mRNA were 46% for β_1 ABKO and 55% for β_1 WT; 55% for β_2 ABKO and 45% for β_2 WT; and 0.02% for β_3 ABKO and 0.04% for β_3 WT ($n = 3$; $P = $ NS). The β_1 and β_2 mRNAs per unit RNA were also the same in ABKO and WT myocytes by RNase protection ($n = 3$; data not shown). The values for ISO stimulation of cAMP in myocytes (maximum fmol cAMP/20,000 cells) were $9,261 \pm 646$ for ABKO and $20,322 \pm 1,765$ for WT (2 curves with 7 doses plus vehicle; $P < 0.05$). The EC_{50} for ISO stimulation of cAMP in myocytes was 33 nM (14–76 nM) for ABKO and 22 nM (8–63 nM) for WT (2 curves; $P = $ NS).

Downregulated cAMP signaling in myocytes was not corrected by inactivation of $G\alpha i$ with pertussis toxin (PTX) (Figure 7B), and forskolin-stimulated cAMP was identical in ABKO and WT myocytes, suggesting normal postreceptor signaling. The cAMP (fmol/20,000 cells) with ISO plus PTX was 15,033 for ABKO and 42,923 for WT ($n = 2$). The cAMP with forskolin was 64,367 for ABKO and 65,696 for WT ($n = 2$). Also, by Western blot, G proteins in myocytes (GRK2, GRK2/3, $G\alpha s$, $G\alpha o$, $G\alpha q$, and $G\beta$) were mildly reduced (data not shown), in proportion to the 25% reduction in myocyte size (1).

In summary, these data show clearly that β-AR protein and mRNA levels and cAMP signaling were not increased in the ABKO heart and myocytes prior to TAC, but that, instead, β-AR function was desensitized in ABKO heart and downregulated in ABKO myocytes. Interestingly, female ABKO mice also had desensitization of ISO-stimulated contraction, even though female ABKO mice are less affected than male ABKO mice (1), and female mice of both genotypes were less sensitive to ISO than males of both genotypes. In female mouse hearts stimu-
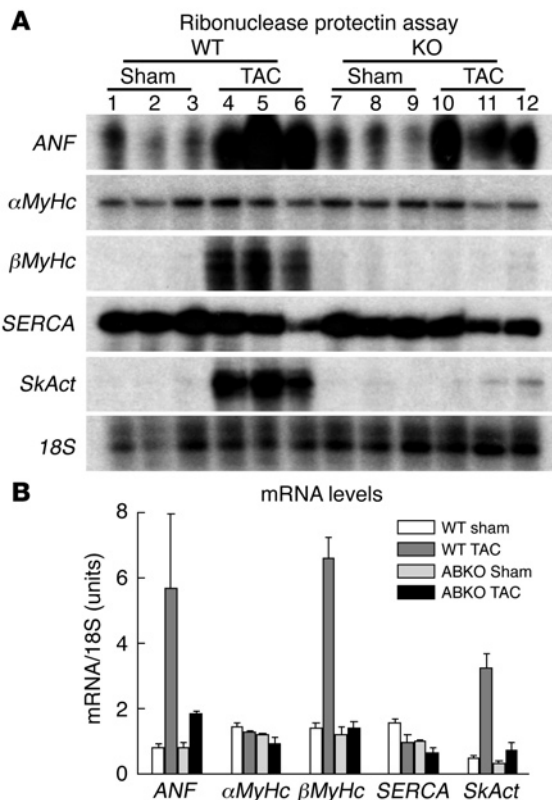
heart, the EC_{50} for ISO stimulation of LVSP (with 95% confidence limits) was 4 nM (2–8 nM) for ABKO ($n = 7$) and 0.8 nM (0.5–1 nM) for WT ($n = 6$; $P < 0.0001$). The EC_{50} for LVEDP was 3 nM (1–7 nM) for ABKO ($n = 7$) and 0.4 nM (0.2–0.8 nM) for WT ($n = 6$; $P < 0.0001$). However, heart levels of GRK2 (βARK1) and $G\beta$ were unchanged by Western blot (data not shown). Thus, the ABKO heart had β-AR desensitization without changes in β-AR levels or some signaling components.

In contrast with heart, ABKO myocytes had a significant 44% reduction in β-AR binding normalized per cell, a significant 54% decrease in maximum ISO-stimulated cAMP per myocyte, with no significant change in the EC_{50}, and a 50% reduction in ISO-stimulated phosphorylation of phospholamban on serine 16, the

A

Ribonuclease protectin assay

B

Figure 4
Fetal gene induction after TAC. (**A**) Total RNA extracted from 3 hearts in each group 4 weeks after TAC or sham surgery was used in ribonuclease protection assay for *ANF*, *αMyHC*, *βMyHC*, *SERCA*, *SkAct*, and 18S RNAs. (**B**) PhosphorImager values for the mRNA levels in **A**, normalized to 18S.

cyte mass were preserved in the ABKO, but several cellular mechanisms were activated that might have contributed to the worse ABKO cardiomyopathy, including failed myocyte gene induction, increased myocyte apoptosis, increased interstitial fibrosis, and β-AR desensitization. As discussed below, each of these mechanisms can be related to the absence of α_1-ARs in myocytes. Therefore, these results define an adaptive and protective role for α_1-ARs after a pathological stimulus to cardiac hypertrophy.

The results have 2 important clinical implications. First, they suggest a plausible mechanism for the harmful cardiac outcomes with α_1-antagonists in the ALLHAT and V-HeFT clinical trials (5, 9). Our data suggest that the loss of adaptive α_1-AR signaling in cardiac myocytes might underlie the adverse outcomes in ALLHAT and V-HeFT, and that these outcomes are not nonspecific drug effects (11). In this regard, the results emphasize concern about the widespread use of α_1-antagonists to treat hypertension or prostate enlargement (14), especially in patients with heart disease. Extrapolation from mice to humans is considered problematic, but KO mice are in fact proving to be effective predictors of drug effects in humans (39). Therefore, the parallel is noteworthy between the adverse cardiac outcomes in the α_1-antagonist patients in the ALLHAT trial and in the ABKO mice. A second clinical implication of our results is that the neurohormonal paradigm of sympathetic toxicity in heart failure should be reassessed. Indeed, adverse outcomes with doxazosin in ALLHAT and with NE reduction in the Moxonidine Safety and Efficacy (MOXSE) trial, the Moxonidine Congestive Heart Failure (MOXCON) trial, and the Beta-Blocker Evaluation of Survival Trial (BEST) (40–42) have raised concerns about

lated with ISO, the EC_{50} for ISO stimulation of LVSP was 18 nM (8–38 nM) for ABKO ($n = 6$) and 5 nM (2–13 nM) for WT ($n = 5$; $P < 0.004$). The EC_{50} for LVEDP in females was 10 nM (6–19 nM) for ABKO ($n = 6$) and 4 nM (2–8 nM) for WT ($n = 5$; $P < 0.0001$).

Locomotor activity. To test whether baseline differences in physical activity might have altered the ABKO response to TAC or changed β-AR signaling, we measured home cage locomotion continuously for 3 days. There were no differences in locomotor activity levels in ABKO versus WT mice ($n = 8$–9 per genotype, data not shown).

Discussion

The key finding of this study is that deletion of the α_{1A}- and α_{1B}-AR subtypes in the ABKO heart caused a maladaptive response to pressure overload. Pressure overload by TAC in the ABKO resulted in high mortality due to heart failure, and a worse dilated cardiomyopathy, with more depressed ejection fraction and larger ventricular volumes. Thus, the ABKO phenotype after TAC was a more maladaptive pathological hypertrophy. Increases in heart and myo-

Figure 5
Apoptosis in heart. (**A**) Hearts at 2 weeks after TAC or sham surgery were analyzed by TUNEL staining. TUNEL-positive nuclei in TAC hearts are stained pink (arrows); membranes are green (FITC-conjugated wheat germ agglutinin), and nuclei are blue (Hoechst 33342). Magnification, ×400. (**B**) TUNEL staining was quantified in 3,000 nuclei from 10 or more randomly selected fields per heart. Numbers of hearts are indicated, and matched areas from the LV, IVS, and RV were sampled in every heart. (**C**) Phospho-PKCδ was assayed 1 week after TAC or sham surgery by Western blot on extracts from 3 hearts per group. An antibody against total PKCδ gave the same pattern, but background was higher (data not shown). Full-length and cleaved PKCδ are indicated.

A

TUNEL stain

B

C

PKCδ
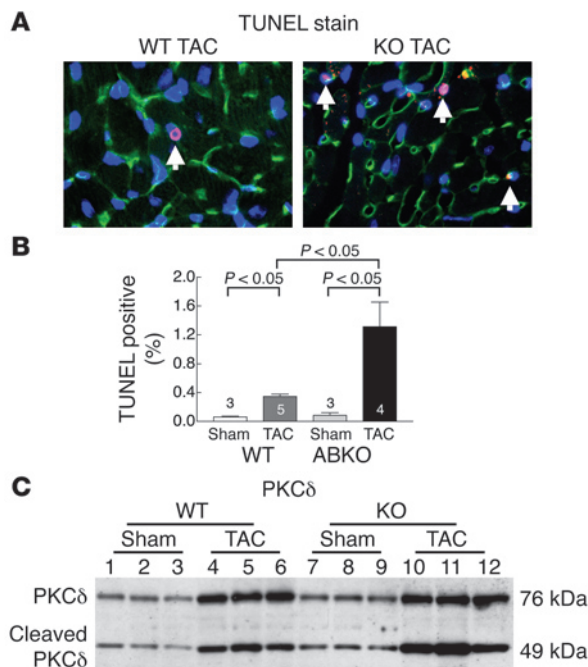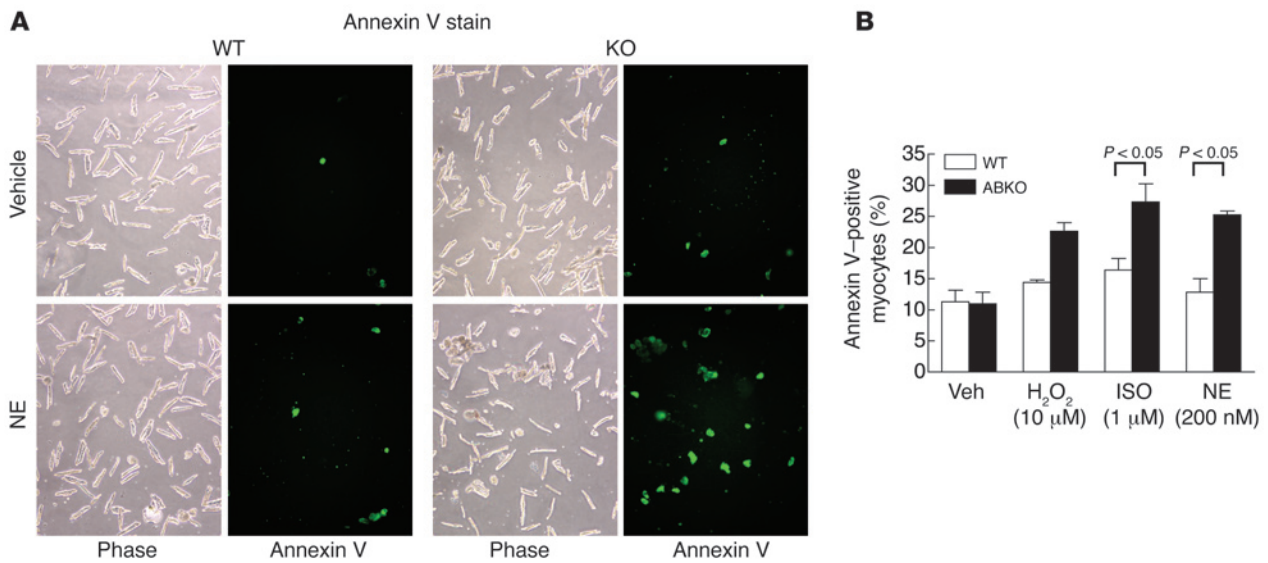
Figure 6
Apoptosis in cultured myocytes. (**A**) Cultured adult mouse myocytes from WT and ABKO hearts without prior TAC were treated for 2 hours with 200 nM NE or vehicle and visualized by phase-contrast or fluorescence microscopy for annexin V staining, a marker for apoptosis. Magnification, ×100. Note for ABKO myocytes the overall smaller myocyte size by phase contrast and the increased annexin V staining after NE. (**B**) Annexin V–positive myocytes were quantified as percentage of total myocytes after treatment for 2 hours with 10 μM H_2O_2, 1 μM ISO, or 200 nM NE. Values are from 2 (H_2O_2) or 3 (ISO, NE) experiments with myocytes from different hearts.

the limits of sympathetic inhibition in heart failure (15–18). Our results raise the intriguing possibility that sympathetic *activation* of α_1-ARs might be beneficial in heart failure.

We identified several potential cellular mechanisms of worse dilated cardiomyopathy in the ABKO, involving gene transcription, apoptosis, fibrosis, and β-ARs. Each of these cellular mechanisms could be predicted from the known actions of α_1-ARs in myocytes, suggesting a direct link between the KO and the phenotype.

Impaired transcription of sarcomeric genes could explain the characteristic finding of reduced myofibrils in myocytes from human and animal cardiomyopathy (43–45), and $\beta MyHC$ and other sarcomeric mRNAs are reduced in the failing human heart and are rescued by LV assist device therapy (46, 47). In the ABKO heart after TAC, impaired induction was most prominent for the highly induced fetal genes *ANF*, $\beta MyHC$, and *SkAct*, but there was also a trend to lower $\alpha MyHC$ and *SERCA* (Figure 4 and Table 1), consistent with the observation that α_1-ARs activate transcription in cultured cardiac myocytes of both constitutive and inducible mRNAs, plus ribosomal and transfer RNAs (48). α_1-ARs were the first receptors linked to fetal gene induction in a model of cardiac hypertrophy (48–50), and α_1-stimulation is used widely to study transcriptional regulation. The present results show that no other receptor(s) can compensate to activate fetal genes when α_1-ARs are missing.

Apoptosis is now recognized as one mechanism of cardiomyopathy (29, 30). Increased apoptosis in the ABKO heart after TAC and in ABKO myocytes (Figures 5 and 6) is explainable by acute and chronic effects of α_1-signaling. Acute α_1-AR inhibition of myocyte apoptosis is well documented (51–54), and the mechanisms include activating Erk and inactivating BAD, stimulating adenosine production, increasing glucose metabolism, and reducing intracellular acidity (3, 4). Besides these acute effects, α_1-ARs chronically upregulate antiapoptotic factors, such as superoxide dismutase and iNOS (55, 56). Similarly, preliminary DNA array experiments identify several genes related to apoptosis that are regulated significantly in α_1-AR KO myocytes (P. Simpson et al., unpublished observations). Thus, increased apoptosis in the ABKO has multiple likely mechanisms.

Interstitial and perivascular fibrosis are characteristic of cardiomyopathy (26), but only interstitial fibrosis was greater in the ABKO heart after TAC (Figure 3C). Increased interstitial fibrosis can be explained by paracrine mechanisms, since α_1-ARs are not expressed in cardiac fibroblasts (57). First, *ANF* induction was markedly less in the ABKO after TAC (Figure 4), and the natriuretic peptides inhibit fibrosis by direct effects on fibroblasts (58–62). Thus, impaired upregulation of ANF could partly explain increased fibrosis. Second, increased apoptosis in the ABKO could itself contribute to increased fibrosis, since cardiac interstitial fibrosis is observed in models where apoptosis is the primary mechanism (30), and apoptosis is recognized as a cause of interstitial fibrosis in other organs (63, 64).

Finally, β-ARs were desensitized in the ABKO heart, even before pressure overload (Figure 7). Myocyte β-AR desensitization is a classical finding in early cardiomyopathy and heart failure but might be a double-edged sword, protecting against β-AR–mediated apoptosis but also reducing adaptive β-AR contractile effects (65). Interestingly, ABKO myocytes had increased β-AR–mediated apoptosis, even when β-ARs and signaling were downregulated (Figures 6 and 7). β-AR desensitization in the ABKO heart might have been caused by a classical mechanism of β-AR phosphorylation and internalization (66), perhaps secondary to increased sympathetic activity in the ABKO from reduced cardiac output (1), as observed in the single α_{1A}-AR KO (67). Alternately, β-AR desensitization in the ABKO heart might have been caused by the reduction in β-AR levels and β-mediated cAMP and protein kinase A signaling in each ABKO myocyte (Figure 7). Although
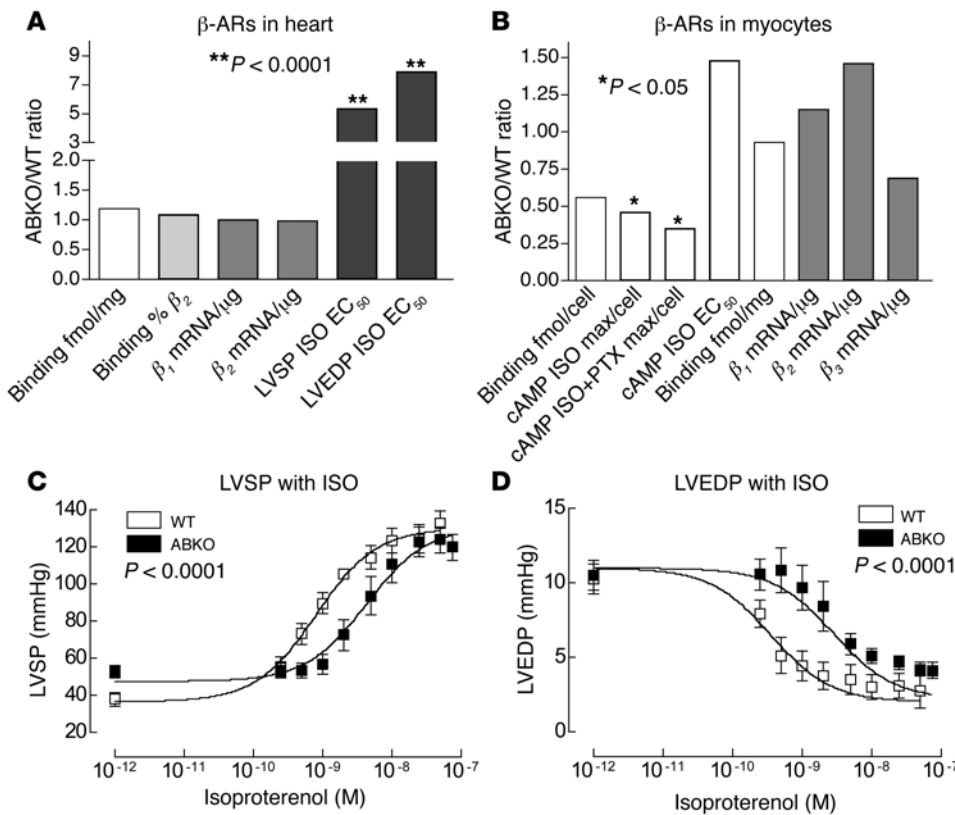
Figure 7
β-ARs in heart and myocytes. (**A** and **B**) β-AR mRNA and protein levels and cAMP signaling were assayed in ABKO hearts (**A**) and isolated myocytes (**B**) without prior TAC, and ratios of mean values are plotted (ABKO/WT). (**C** and **D**) Dose-response curves for ISO stimulation of LVSP (**C**) and LVEDP (**D**). The ratios of EC_{50} values are plotted in **A**. See Results for absolute values.

failure, and it is highly pertinent in this regard that an α_1-agonist can prevent doxorubicin cardiotoxicity in mice (74). A first step to test α_1-agonist therapy rationally is to discover whether the A, the B, or both are responsible primarily for the ABKO phenotype. Preliminary data suggest that the A subtype can rescue the apoptosis phenotype in ABKO myocytes, but the B subtype cannot (T. O'Connell et al., unpublished observations), pointing to a role of the A in apoptosis, and also showing that systemic factors do not cause the increased susceptibility to apoptosis.

In summary, double KO of the α_{1A}- and α_{1B}-AR subtypes caused a maladaptive response to pressure overload, through multiple cellular mechanisms. These results suggest caution in the use of α_1-antagonists, especially in patients with cardiovascular disease. By suggesting that α_1-AR activation might be beneficial and adaptive, the results also provide an alternate insight into the neurohormonal paradigm in heart failure and raise the possibility that α_1-AR agonists might be therapeutic candidates in heart failure.

ABKO myocytes had unchanged β-AR proteins and mRNAs per unit of protein or RNA (Figure 7B), the total heart β-ARs would have been reduced, simply because the myocytes were smaller.

In summary, the cause of worse cardiomyopathy in the ABKO was likely multifactorial, including failed myocyte gene induction, increased myocyte apoptosis, increased interstitial fibrosis, and β-AR desensitization. Another possibility not tested is that the ABKO impaired myocyte renewal, a possibility based on the fact that bone marrow mesenchymal stem cells express α_1-ARs before differentiation into cardiomyocytes (68).

A phenotype qualitatively similar to that of the ABKO, impaired growth in a model of "physiological" hypertrophy (normal development) associated with a more maladaptive response in a model of "pathological" hypertrophy (aortic constriction), is also observed in genetic mouse models with reduced insulin receptor/PI3K signaling (69–73). These phenotypes suggest that different signaling pathways regulate physiological and pathological hypertrophy. However, α_1-ARs and insulin receptors regulate distinct signaling modules, at least in part, since α_1-ARs activate Erk, whereas the insulin receptor activates PI3K. Thus, α_1-ARs might be one of a few key mechanisms for physiological hypertrophy signaling, which might be beneficial to activate and harmful to inhibit. It will be important to test whether activation of the different physiological hypertrophy signaling pathways can be used to treat pathological hypertrophy and heart

Methods

Mice. α_{1A}-AR and α_{1B}-AR double KO (ABKO) mice were generated as described previously (1). Most experiments used sixth- and seventh-generation congenic male C57BL/6J mice, age 10–12 weeks. Mice with KO of β_1-ARs or β_2-ARs were a generous gift of Daniel Bernstein (Stanford University, Stanford, California, USA) (75). Animal care and use in these experiments was approved by the Animal Care Committees at the San Francisco Veterans Affairs Medical Center and the University of South Dakota (Vermillion, South Dakota, USA).

Transverse aortic constriction. TAC was done without intubation under anesthesia with isoflurane (1), and the surgeon was blinded to genotype. The pressure gradient across the stenosis at 2 weeks was estimated by echocardiography in conscious mice, which predicts the gradient measured by catheterization (19).

Echocardiography. Echocardiography was performed on conscious, gently restrained mice, with an Acuson Sequoia C256 (Siemens) using a 15-MHz linear array transducer, and ventricular dimensions were measured from 2-dimensionally guided M-mode echocardiograms (19, 76). The echocardiographer was blinded to genotype.

Heart histology. Hearts were cannulated through the LV apex in situ, cleared by perfusion with PBS at 70 mmHg, arrested in diastole with 60 mM KCl, fixed by perfusion with 4% paraformaldehyde, embedded in paraffin, and sectioned at 8 μm. For myocyte cross-sectional area, coronal sections were deparaffinized and stained for membranes with fluorescein-conjugated wheat germ agglutinin (Invitrogen Corp.) and for nuclei with Hoechst

33342 (Calbiochem), and myocyte area was measured by fluorescence microscopy at ×400 magnification (Nikon Eclipse E600; Nikon Inc.) using NIH Image (1). For fibrosis, coronal sections were stained for collagen with Sirius red and for cells with fast green, and red-stained area was measured by phase microscopy at ×400 magnification (Nikon Eclipse E600) using Image-Pro software (MediaCybernetics). Operators were blinded to genotype and treatment group.

RNase protection assay for myocyte mRNAs. The mRNAs for *MyHC*, *SkAct*, *SERCA*, *ANF*, and *18S* (Ambion Inc.) were detected by ribonuclease protection assay (RPA III; Ambion Inc.) with rat labeled RNA probes, using 3 μg of total ventricular RNA isolated from sham-operated and TAC mice after 4 weeks (TRIzol; Invitrogen Corp.). Bands were quantified using a PhosphorImager (Bio-Rad Laboratories) and normalized to 18S (Ambion Inc.) (77).

Apoptosis in intact heart. Apoptosis was measured by TUNEL assays on paraffin-embedded sections using the ApopTag Red In Situ Apoptosis Detection Kit (Serologicals Corp.), with the exception that sections were treated with 0.1% saponin and 1 mM EGTA before TUNEL staining (31). Counting of TUNEL-positive cells was done blinded to genotype and treatment. PKCδ cleavage was measured in ventricular extracts by Western blot, using antibodies against total PKCδ (no. 610397; BD Biosciences − Clontech) and phospho-PKCδ T505 (no. 9374; Cell Signaling Technology). Bands were detected by chemiluminescence (Amersham Biosciences) and quantified using ImageQuant software (Amersham Biosciences).

Isolation and culture of adult mouse cardiac myocytes. Ventricular myocytes were isolated by perfusion with collagenase, plated at 50 rod-shaped cells per square millimeter on laminin-coated 35-mm dishes or 2-well slides, and cultured in MEM with HBSS and 0.1 mg/ml BSA at 2% CO_2 and 37°C (1, 78).

Apoptosis in isolated myocytes. Cultured myocytes were treated for 2 hours with agonists, and apoptosis was measured using anti–annexin V antibody (Annexin-V-FLUOS; Roche Diagnostics Corp.). H_2O_2, L-NE bitartrate, L-ISO HCl, and ascorbic acid (vehicle, 100 μM final) were from Sigma-Aldrich.

β-AR binding in hearts and myocytes. Binding assays used both total homogenates of freshly isolated myocytes, and membranes prepared from ventricles and myocytes by homogenization (0.25 M sucrose, 30 mM histidine, 1 mM EDTA [pH 8.0], PMSF, protease inhibitors) and centrifugation twice at 100,000 g (79). Saturation analyses used 0.04–1.2 μM [^{125}I]cyanopindolol (PerkinElmer), with 1 μM DL-propranolol (Sigma-Aldrich) to define nonspecific binding (80). Total receptor number (B_{max}) and binding affinity (K_d) were calculated by nonlinear regression with GraphPad Prism (version 4.0b; GraphPad Software). The percentage β₂-ARs was estimated by competition for [^{125}I]cyanopindolol binding (50 pM) by ICI-118,551 (1 nM–50 μM), using an F test to test whether a 2-site model was significantly better fit than a 1-site model, and to compute the percentage of sites with high affinity for ICI-118,551 (β₂-ARs) (GraphPad Prism version 4.0b; GraphPad Software).

β-AR and G protein Western blot. For β-ARs, membranes were prepared from hearts and myocytes the same as for binding. Membrane proteins (50–100 μg) were resuspended in Tris-EDTA with PMSF and protease inhibitors, and loaded, without boiling, onto 10% SDS-polyacrylamide gels. Membrane proteins for β₂-AR assay were first treated with peptide *N*-glycosidase F, using a kit from New England Biolabs Inc. (no. P0704S) (81, 82). Separated proteins were transferred to nitrocellulose, blocked, and probed with rabbit polyclonal antibodies from Santa Cruz Biotechnology Inc., SC-568 (V-19) for the β₁-AR and SC-570 (M-20) for the β₂-AR. For G proteins, hearts or myocytes were lysed and blotted with antibodies from Santa Cruz Biotechnology Inc. against GRK2 (C-15, sc-562), Gαs (K-20, sc-823), Gαo (K-20, sc-387), Gαq (E-17, sc-262), and Gαi (C-10, sc-262). An antibody against Gβ (06-238) was from Upstate

USA Inc., and an antibody against GRK2/3 (G8972) was from United States Biological Inc.

β-AR mRNAs in heart and myocytes. Ribonuclease protection assay for β₁- and β₂-AR mRNAs used 15 μg total RNA (TRIzol) from hearts or isolated myocytes, with sequence-verified labeled probes. A β₁-AR probe was amplified from a human heart cDNA library (no. 780612; Stratagene) using the following primers: sense at bp 411, 5′-AGATGTGCT-GTGTGTGAC-3′; and antisense at bp 701, 5′-TAGAAGGAGACGACG-GAC-3′. A mouse β₂-AR probe was from Brian Kobilka and Timothy Angelotti (Stanford University, Stanford, California, USA). Quantitative RT-PCR for β₁-, β₂-, and β₃-AR mRNAs used total myocyte RNA (TRIzol and RNeasy Mini Kit; QIAGEN) treated with TURBO DNase (Ambion Inc.). One microgram RNA was reverse-transcribed with oligo-dT primers and SuperScript II Reverse Transcriptase (Invitrogen Corp.). Five percent of the cDNA product was used in quantitative PCR with SYBR Green and an ABI PRISM 7900 Sequence Detection System. PCR was 94°C for 4 minutes, then 35 cycles of 94°C for 2 minutes, 55°C for 1 minute, and 72°C for 2 minutes, followed by 72°C for 10 minutes. Data were analyzed with SDS software version 2.1 (Applied Biosystems). PCR products were also evaluated on gels for primer-dimers or other nonspecific bands, which were further excluded by a dissociation protocol at the end of cycling. β₁-AR primers were validated using tissues from the β₁-AR KO mice (data not shown). Mouse β-AR primers were designed on PrimerQuest (Integrated DNA Technologies Inc.) with accession numbers and coordinates as follows: β₁-AR forward, NM_007419 (641 AGTGCTGCGATTTCGTCAC-CAACA 664); β₁-AR reverse, NM_007419 (787 GCTCGCAGCTGTC-GATCTTCTTTA 764); β₂-AR forward, NM_007420 (912 ATCT-GAAGGAAGATTCCACGCCCA 935); β₂-AR reverse, NM_007420 (1060 AGAGGGTGAATGTGCCCATGATGA 1037); β₃-AR forward, NM_013462 (888 TGCGCACCTTAGGTCTCATTATGG 911); β₃-AR reverse, NM_013462 (998 AAACTCCGCTGGGAACTAGAGAGG 975).

cAMP and phospholamban in myocytes. Myocytes were cultured overnight and treated for 10 minutes with 1 nM–1 μM ISO (7 doses) or vehicle, with duplicate dishes for each dose in each experiment. Intracellular cAMP was extracted and assayed by ELISA (Biotrak; Amersham Biosciences). Curves were fit to sigmoidal dose-response curves and compared with an F test (GraphPad Prism version 4.0b; GraphPad Software). Some cultures were pretreated with 1 μg/ml PTX (List Biological Laboratories Inc.) for 12–16 hours at 37°C, then stimulated with 1 μM ISO for 10 minutes. Other cultures were treated with 1 μM forskolin (Sigma-Aldrich) for 10 minutes. Phospholamban phosphorylation after treatment of cultured myocytes with 1 μM ISO was measured by Western blot with anti–phospho-phospholamban S16 (no. 07-052; Upstate USA Inc.).

β-AR–mediated contractility in isolated hearts. Isolated hearts were paced at 9 Hz and perfused retrograde through the aorta at 70 mmHg pressure and 37°C with modified Krebs-Henseleit buffer containing 1.5 mM calcium (83). LV pressure was monitored with a fluid-filled balloon inserted via the left atrium (83), while ISO in Krebs-Henseleit was infused from 1 to 50 nM. Data were fit to sigmoidal dose-response curves, and curves were compared with an F test (GraphPad Prism version 4.0b; GraphPad Software).

Locomotor activity. Mice naive to prior testing were housed individually in rat cages (48 × 27 × 13 cm) with bedding, food, and water, under a 12-hour light/dark cycle. To quantify activity, beam breaks were collected continuously for 3 days with a photobeam activity system (Flex-Field; San Diego Instruments) (84).

Data analysis. Results are mean ± SEM. Mean values were compared by ANOVA for groups of 4, with the Bonferroni post-test comparison, or by the unpaired 2-tailed Student's *t* test for 2 groups. *P* values less than 0.05 were considered significant.

Address correspondence to: Paul C. Simpson, San Francisco VA Medical Center 111C8, 4150 Clement Street, San Francisco, California 94121, USA. Phone: (415) 221-4810 ext. 3200; Fax: (415) 379-5570; E-mail: paul.simpson@ucsf.edu.

Timothy D. O'Connell's present address is: Cardiovascular Research Institute, South Dakota Health Research Foundation and Department of Medicine, The University of South Dakota, Vermillion, South Dakota, USA.
Lynne Turnbull's present address is: Microbiology Department, Monash University, Victoria, Australia.

Shinji Ishizaka's present address is: Second Department of Internal Medicine, Toyama Medical and Pharmaceutical University, Toyama, Japan.

1. O'Connell, T.D., et al. 2003. The α(1a/c)- and α(1b)-adrenergic receptors are required for physiological cardiac hypertrophy in the double-knockout mouse. *J. Clin. Invest.* **111**:1783–1791. doi:10.1172/JCI200316100.
2. McCloskey, D.T., et al. 2003. Abnormal myocardial contraction in alpha(1a)- and alpha(1b)-adrenoceptor double-knockout mice. *J. Mol. Cell. Cardiol.* **35**:1207–1216.
3. Mani, K., Ashton, A.W., and Kitsis, R.N. 2002. Taking the bad out of adrenergic stimulation. *J. Mol. Cell. Cardiol.* **34**:709–712.
4. Salvi, S. 2001. Protecting the myocardium from ischemic injury: a critical role for alpha(1)-adrenoreceptors? *Chest.* **119**:1242–1249.
5. ALLHAT Collaborative Research Group. 2000. Major cardiovascular events in hypertensive patients randomized to doxazosin vs chlorthalidone: the antihypertensive and lipid-lowering treatment to prevent heart attack trial (ALLHAT). *JAMA.* **283**:1967–1975.
6. Davis, B.R., et al. 2002. Relationship of antihypertensive treatment regimens and change in blood pressure to risk for heart failure in hypertensive patients randomly assigned to doxazosin or chlorthalidone: further analyses from the antihypertensive and lipid-lowering treatment to prevent heart attack trial. *Ann. Intern. Med.* **137**:313–320.
7. Piller, L.B., et al. 2002. Validation of heart failure events in the Antihypertensive and Lipid Lowering Treatment to Prevent Heart Attack Trial (ALLHAT) participants assigned to doxazosin and chlorthalidone. *Curr. Control. Trials Cardiovasc. Med.* **3**:10.
8. ALLHAT Collaborative Research Group. 2003. Diuretic versus alpha-blocker as first-step antihypertensive therapy: final results from the Antihypertensive and Lipid-Lowering Treatment to Prevent Heart Attack Trial (ALLHAT). *Hypertension.* **42**:239–246.
9. Cohn, J.N. 1993. The Vasodilator-Heart Failure Trials (V-HeFT). Mechanistic data from the VA Cooperative Studies. Introduction. *Circulation.* **87**:VI1–VI4.
10. Anglin, I.E., Glassman, D.T., and Kyprianou, N. 2002. Induction of prostate apoptosis by alpha1-adrenoceptor antagonists: mechanistic significance of the quinazoline component. *Prostate Cancer Prostatic Dis.* **5**:88–95.
11. Gonzalez-Juanatey, J.R., Iglesias, M.J., Alcaide, C., Pineiro, R., and Lago, F. 2003. Doxazosin induces apoptosis in cardiomyocytes cultured in vitro by a mechanism that is independent of alpha1-adrenergic blockade. *Circulation.* **107**:127–131.
12. Weinshank, R.L., et al. 1990. Cloning, expression, and pharmacological characterization of a human alpha 2b-adrenergic receptor. *Mol. Pharmacol.* **38**:681–688.
13. Bylund, D.B., et al. 1992. Pharmacological characteristics of alpha 2-adrenergic receptors: comparison of pharmacologically defined subtypes with subtypes identified by molecular cloning. *Mol. Pharmacol.* **42**:1–5.
14. Vaughan, E.D., Jr. 2003. Medical management of benign prostatic hyperplasia: are two drugs better than one? *N. Engl. J. Med.* **349**:2449–2451.
15. Cohn, J.N. 2002. Sympathetic nervous system in heart failure. *Circulation.* **106**:2417–2418.
16. Bristow, M. 2003. Antiadrenergic therapy of chronic heart failure: surprises and new opportunities. *Circulation.* **107**:1100–1102.
17. Gottlieb, S.S. 2003. The neurohormonal paradigm: have we gone too far? *J. Am. Coll. Cardiol.* **41**:1458–1459.
18. Mehra, M.R., Uber, P.A., and Francis, G.S. 2003. Heart failure therapy at a crossroad: are there limits to the neurohormonal model? *J. Am. Coll. Cardiol.* **41**:1606–1610.
19. Nakamura, A., et al. 2001. LV systolic performance improves with development of hypertrophy after transverse aortic constriction in mice. *Am. J. Physiol. Heart Circ. Physiol.* **281**:H1104–H1112.
20. The SOLVD Investigators. 1991. Effect of enalapril on survival in patients with reduced left ventricular ejection fractions and congestive heart failure. *N. Engl. J. Med.* **325**:293–302.
21. The SOLVD Investigators. 1992. Effect of enalapril on mortality and the development of heart failure in asymptomatic patients with reduced left ventricular ejection fractions. *N. Engl. J. Med.* **327**:685–691.
22. Wong, M., et al. 2004. Severity of left ventricular remodeling defines outcomes and response to therapy in heart failure: Valsartan heart failure trial (Val-HeFT) echocardiographic data. *J. Am. Coll. Cardiol.* **43**:2022–2027.
23. Koide, M., et al. 1997. Premorbid determinants of left ventricular dysfunction in a novel model of gradually induced pressure overload in the adult canine. *Circulation.* **95**:1601–1610.
24. Badorff, C., et al. 2002. Fas receptor signaling inhibits glycogen synthase kinase 3 β and induces cardiac hypertrophy following pressure overload. *J. Clin. Invest.* **109**:373–381. doi:10.1172/JCI200213779.
25. Gunther, S., and Grossman, W. 1979. Determinants of ventricular function in pressure-overload hypertrophy in man. *Circulation.* **59**:679–688.
26. Weber, K.T., and Brilla, C.G. 1991. Pathological hypertrophy and cardiac interstitium. Fibrosis and renin-angiotensin-aldosterone system. *Circulation.* **83**:1849–1865.
27. Lindsey, M.L., et al. 2003. Effect of a cleavage-resistant collagen mutation on left ventricular remodeling. *Circ. Res.* **93**:238–245.
28. Simpson, P.C., Long, C.S., Waspe, L.E., Henrich, C.J., and Ordahl, C.P. 1989. Transcription of early developmental isogenes in cardiac myocyte hypertrophy. *J. Mol. Cell. Cardiol.* **21**(Suppl. 5):79–89.
29. Kang, P.M., and Izumo, S. 2003. Apoptosis in heart: basic mechanisms and implications in cardiovascular diseases. *Trends Mol. Med.* **9**:177–182.
30. Wencker, D., et al. 2003. A mechanistic role for cardiac myocyte apoptosis in heart failure. *J. Clin. Invest.* **111**:1497–1504. doi:10.1172/JCI200317664.
31. Kubota, T., et al. 2001. Overexpression of tumor necrosis factor-alpha activates both anti- and proapoptotic pathways in the myocardium. *J. Mol. Cell. Cardiol.* **33**:1331–1344.
32. Bayer, A.L., et al. 2003. Alterations in protein kinase C isoenzyme expression and autophosphorylation during the progression of pressure overload-induced left ventricular hypertrophy. *Mol. Cell. Biochem.* **242**:145–152.
33. Narula, J., et al. 1999. Apoptosis in heart failure: release of cytochrome c from mitochondria and activation of caspase-3 in human cardiomyopathy. *Proc. Natl. Acad. Sci. U. S. A.* **96**:8144–8149.
34. Byrne, J.A., et al. 2003. Contrasting roles of NADPH oxidase isoforms in pressure-overload versus angiotensin II–induced cardiac hypertrophy. *Circ. Res.* **93**:802–805.
35. Ide, T., et al. 2000. Direct evidence for increased hydroxyl radicals originating from superoxide in the failing myocardium. *Circ. Res.* **86**:152–157.
36. Cohn, J.N., et al. 1984. Plasma norepinephrine as a guide to prognosis in patients with chronic congestive heart failure. *N. Engl. J. Med.* **311**:819–823.
37. Ostman-Smith, I. 1981. Cardiac sympathetic nerves as the final common pathway in the induction of adaptive cardiac hypertrophy. *Clin. Sci. (Lond.)* **61**:265–272.
38. Hagemann, D., and Xiao, R.P. 2002. Dual site phospholamban phosphorylation and its physiological relevance in the heart. *Trends Cardiovasc. Med.* **12**:51–56.
39. Zambrowicz, B.P., and Sands, A.T. 2003. Knockouts model the 100 best-selling drugs: will they model the next 100? *Nat. Rev. Drug Discov.* **2**:38–51.
40. Swedberg, K., et al. 2002. Effects of sustained-release moxonidine, an imidazoline agonist, on plasma norepinephrine in patients with chronic heart failure. *Circulation.* **105**:1797–1803.
41. Coats, A.J. 1999. Heart failure 99: the MOXCON story. *Int. J. Cardiol.* **71**:109–111.
42. Bristow, M.R., et al. 2004. Effect of baseline or changes in adrenergic activity on clinical outcomes in the beta-blocker evaluation of survival trial. *Circulation.* **110**:1437–1442.
43. Schwarz, F., et al. 1981. Reduced volume fraction of myofibrils in myocardium of patients with decompensated pressure overload. *Circulation.* **63**:1299–1304.
44. Zimmer, G., et al. 1992. Decreased concentration of myofibrils and myofiber hypertrophy are structural determinants of impaired left ventricular function in patients with chronic heart diseases:

a multiple logistic regression analysis. *J. Am. Coll. Cardiol.* **20**:1135–1142.

45. Kostin, S., et al. 2003. Myocytes die by multiple mechanisms in failing human hearts. *Circ. Res.* **92**:715–724.

46. Razeghi, P., et al. 2001. Metabolic gene expression in fetal and failing human heart. *Circulation.* **104**:2923–2931.

47. Rodrigue-Way, A., et al. 2005. Sarcomeric genes involved in reverse remodeling of the heart during left ventricular assist device support. *J. Heart Lung Transplant.* **24**:73–80.

48. Long, C.S., Ordahl, C.P., and Simpson, P.C. 1989. α 1-Adrenergic receptor stimulation of sarcomeric actin isogene transcription in hypertrophy of cultured rat heart muscle cells. *J. Clin. Invest.* **83**:1078–1082.

49. Bishopric, N.H., Simpson, P.C., and Ordahl, C.P. 1987. Induction of the skeletal α-actin gene in α 1-adrenoceptor-mediated hypertrophy of rat cardiac myocytes. *J. Clin. Invest.* **80**:1194–1199.

50. Waspe, L.E., Ordahl, C.P., and Simpson, P.C. 1990. The cardiac beta-myosin heavy chain isogene is induced selectively in α 1-adrenergic receptor-stimulated hypertrophy of cultured rat heart myocytes. *J. Clin. Invest.* **85**:1206–1214.

51. Iwai-Kanai, E., et al. 1999. Alpha- and beta-adrenergic pathways differentially regulate cell type-specific apoptosis in rat cardiac myocytes. *Circulation.* **100**:305–311.

52. Valks, D.M., et al. 2002. Phenylephrine promotes phosphorylation of Bad in cardiac myocytes through the extracellular signal-regulated kinases 1/2 and protein kinase A. *J. Mol. Cell. Cardiol.* **34**:749–763.

53. Zhu, H., McElwee-Witmer, S., Perrone, M., Clark, K.L., and Zilberstein, A. 2000. Phenylephrine protects neonatal rat cardiomyocytes from hypoxia and serum deprivation-induced apoptosis. *Cell Death Differ.* **7**:773–784.

54. De Windt, L.J., et al. 2000. Calcineurin-mediated hypertrophy protects cardiomyocytes from apoptosis in vitro and in vivo: an apoptosis-independent model of dilated heart failure. *Circ. Res.* **86**:255–263.

55. Amin, J.K., et al. 2001. Reactive oxygen species mediate alpha-adrenergic receptor-stimulated hypertrophy in adult rat ventricular myocytes. *J. Mol. Cell. Cardiol.* **33**:131–139.

56. Tejero-Taldo, M.I., Gursoy, E., Zhao, T.C., and Kukreja, R.C. 2002. Alpha-adrenergic receptor stimulation produces late preconditioning through inducible nitric oxide synthase in mouse heart. *J. Mol. Cell. Cardiol.* **34**:185–195.

57. Stewart, A.F., et al. 1994. Cloning of the rat alpha 1c-adrenergic receptor from cardiac myocytes. Alpha 1c, alpha 1b, and alpha 1d mRNAs are present in cardiac myocytes but not in cardiac fibroblasts. *Circ. Res.* **75**:796–802.

58. Hanford, D.S., Thuerauf, D.J., Murray, S.F., and Glembotski, C.C. 1994. Brain natriuretic peptide is induced by alpha 1-adrenergic agonists as a primary response gene in cultured rat cardiac myocytes. *J. Biol. Chem.* **269**:26227–26233.

59. Cao, L., and Gardner, D.G. 1995. Natriuretic peptides inhibit DNA synthesis in cardiac fibroblasts. *Hypertension.* **25**:227–234.

60. Redondo, J., Bishop, J.E., and Wilkins, M.R. 1998. Effect of atrial natriuretic peptide and cyclic GMP phosphodiesterase inhibition on collagen synthesis by adult cardiac fibroblasts. *Br. J. Pharmacol.* **124**:1455–1462.

61. Calderone, A., Thaik, C.M., Takahashi, N., Chang, D.L., and Colucci, W.S. 1998. Nitric oxide, atrial natriuretic peptide, and cyclic GMP inhibit the growth-promoting effects of norepinephrine in cardiac myocytes and fibroblasts. *J. Clin. Invest.* **101**:812–818.

62. Tamura, N., et al. 2000. Cardiac fibrosis in mice lacking brain natriuretic peptide. *Proc. Natl. Acad. Sci. U. S. A.* **97**:4239–4244.

63. Kuwano, K., Hagimoto, N., and Nakanishi, Y. 2004. The role of apoptosis in pulmonary fibrosis. *Histol. Histopathol.* **19**:867–881.

64. Canbay, A., Friedman, S., and Gores, G.J. 2004. Apoptosis: the nexus of liver injury and fibrosis. *Hepatology.* **39**:273–278.

65. Lohse, M.J., Engelhardt, S., and Eschenhagen, T. 2003. What is the role of beta-adrenergic signaling in heart failure? *Circ. Res.* **93**:896–906.

66. Perrino, C., et al. 2005. Restoration of beta-adrenergic receptor signaling and contractile function in heart failure by disruption of the betaark1/phosphoinositide 3-kinase complex. *Circulation.* **111**:2579–2587.

67. Rokosh, D.G., and Simpson, P.C. 2002. Knockout of the alpha 1a/c-adrenergic receptor subtype: the alpha 1a/c is expressed in resistance arteries and is required to maintain arterial blood pressure. *Proc. Natl. Acad. Sci. U. S. A.* **99**:9474–9479.

68. Hakuno, D., et al. 2002. Bone marrow-derived regenerated cardiomyocytes (CMG cells) express functional adrenergic and muscarinic receptors. *Circulation.* **105**:380–386.

69. Shioi, T., et al. 2000. The conserved phosphoinositide 3-kinase pathway determines heart size in mice. *EMBO J.* **19**:2537–2548.

70. Belke, D.D., et al. 2002. Insulin signaling coordinately regulates cardiac size, metabolism, and contractile protein isoform expression. *J. Clin. Invest.* **109**:629–639. doi:10.1172/JCI200213946.

71. Crackower, M.A., et al. 2002. Regulation of myocardial contractility and cell size by distinct PI3K-PTEN signaling pathways. *Cell.* **110**:737–749.

72. McMullen, J.R., et al. 2003. Phosphoinositide 3-kinase(p110alpha) plays a critical role for the induction of physiological, but not pathological, cardiac hypertrophy. *Proc. Natl. Acad. Sci. U. S. A.* **100**:12355–12360.

73. Hu, P., et al. 2003. Minimally invasive aortic banding in mice: effects of altered cardiomyocyte insulin signaling during pressure overload. *Am. J. Physiol.*
Heart Circ. Physiol. **285**:H1261–H1269.

74. Aries, A., Paradis, P., Lefebvre, C., Schwartz, R.J., and Nemer, M. 2004. Essential role of gata-4 in cell survival and drug-induced cardiotoxicity. *Proc. Natl. Acad. Sci. U. S. A.* **101**:6975–6980.

75. Bernstein, D., et al. 2005. Differential cardioprotective/cardiotoxic effects mediated by beta-adrenergic receptor subtypes. *Am. J. Physiol. Heart Circ. Physiol.* **289**:H2441–H2449.

76. Ishizaka, S., et al. 2004. New technique for measurement of left ventricular pressure in conscious mice. *Am. J. Physiol. Heart Circ. Physiol.* **286**:H1208–H1215.

77. Deng, X.F., Rokosh, D.G., and Simpson, P.C. 2000. Autonomous and growth factor-induced hypertrophy in cultured neonatal mouse cardiac myocytes. Comparison with rat. *Circ. Res.* **87**:781–788.

78. O'Connell, T.D., Rodrigo, M.C., and Simpson, P.C. 2006. Isolation and culture of adult mouse cardiac myocytes. In *Cardiovascular proteomics: methods and protocols.* F. Vivanco, editor. Humana Press. Totowa, New Jersey, USA. In press.

79. Rokosh, D.G., et al. 1996. Alpha1-adrenergic receptor subtype mRNAs are differentially regulated by alpha1-adrenergic and other hypertrophic stimuli in cardiac myocytes in culture and in vivo. Repression of alpha1b and alpha1d but induction of alpha1c. *J. Biol. Chem.* **271**:5839–5843.

80. Rohrer, D.K., et al. 1996. Targeted disruption of the mouse beta1-adrenergic receptor gene: developmental and cardiovascular effects. *Proc. Natl. Acad. Sci. U. S. A.* **93**:7375–7380.

81. Rybin, V.O., Xu, X., Lisanti, M.P., and Steinberg, S.F. 2000. Differential targeting of beta-adrenergic receptor subtypes and adenylyl cyclase to cardiomyocyte caveolae. A mechanism to functionally regulate the camp signaling pathway. *J. Biol. Chem.* **275**:41447–41457.

82. Oudit, G.Y., et al. 2003. Phosphoinositide 3-kinase gamma-deficient mice are protected from isoproterenol-induced heart failure. *Circulation.* **108**:2147–2152.

83. Turnbull, L., McCloskey, D.T., O'Connell, T.D., Simpson, P.C., and Baker, A.J. 2003. Alpha 1-adrenergic receptor responses in alpha 1AB-AR knockout mouse hearts suggest the presence of alpha 1D-AR. *Am. J. Physiol. Heart Circ. Physiol.* **284**:H1104–H1109.

84. Rocha, B.A., et al. 2002. Enhanced locomotor, reinforcing, and neurochemical effects of cocaine in serotonin 5-hydroxytryptamine 2c receptor mutant mice. *J. Neurosci.* **22**:10039–10045.

85. Youn, H.J., et al. 1999. Two-dimensional echocardiography with a 15-MHz transducer is a promising alternative for in vivo measurement of left ventricular mass in mice. *J. Am. Soc. Echocardiogr.* **12**:70–75.

86. Liao, Y., et al. 2002. Echocardiographic assessment of LV hypertrophy and function in aortic-banded mice: necropsy validation. *Am. J. Physiol. Heart Circ. Physiol.* **282**:H1703–H1708.